

# Impact of Limb Diameter on Passive Two-Phase Flow in Closed Loop Pulsating Heat Pipes: A Numerical Study

Roshan Devidas Bhagat<sup>1</sup>, Samir Deshmukh<sup>2</sup>,

<sup>1</sup>Symbiosis Skills and Professional University  
Kiwale, Pune, India

[roshan.bhagat@sspu.ac.in](mailto:roshan.bhagat@sspu.ac.in) ; [sjdeshmukh@mitra.ac.in](mailto:sjdeshmukh@mitra.ac.in)

<sup>2</sup>Prof Ram Meghe Institute of Technology & Research  
Badnera, Amravati, India

**Abstract** - This paper represents numerical analysis of liquid vapor slug flow carried out in a single turn closed loop pulsating heat pipe (CLPHP) with different limb diameter. 3D numerical model is developed with design modeler tool and meshing is carried out with the meshing tool available in Ansys Workbench. The numerical model is divided into three sections, evaporator condenser and adiabatic section. The inner diameter (ID) of CLPHP is taken as 2mm. The working fluid is used as water with the filling ratio of 60%. Suitable k- $\epsilon$  model with enhanced wall treatment, thermal effect and curvature correction is considered. The evaporator section is subjected to optimum temperature of 343 K, whereas the condenser is at 298 K. Thermal boundary conditions are applied at evaporator section to predict the behavior of liquid vapor slug flow. About 60,00,000 iterations are performed with smaller time step size of 0.0005 to prevent the divergence in velocity field and to avoid the problem of Courant Number (CFL). The liquid vapor slug flow carries sensible and latent heat towards the condenser section. The contours of liquid volume fraction and wall temperatures are observed. The possibility of dry out conditions are checked with numerical analysis; the complex phenomenon of evaporation and condensation is observed to predict the thermal performance of system suitable for electronics cooling applications.

**Keywords:** Liquid vapor slug, pulsating heat pipe, thermal analysis, thermal performance, electronic cooling

## 1. Introduction

The pulsating heat pipe (PHP) has been emerged as one of the most effective heat exchangers for cooling electronic devices [1]. With miniaturization of electronic devices, these devices are confronted with the problem of overheating, reduced performance and lower lifespan [2]. PHP when compared with conventional heat dissipation technology are able to transfer heat without any external power source [3]. The pulsating heat pipe has wide operating temperature range and can adopt to the environment with high heat flux [4]. The principle operation of PHP is very complex as it involves the phase change of working fluid with growth and extinction of liquid and vapor slug as well as nucleate boiling [5]. In order to understand the thermal performance, several theoretical, experimental and numerical studies were carried out, through these studies it was observed that the performance of PHP depends on geometrical, operating and physical parameters [6-7]. Difference of temperature, density between evaporator and condenser along with gravity are the driving force for the operation of PHP [8-9].

In order to predict the thermal performance and to check the possibility of dry out conditions in PHP, numerical analysis of single turn closed loop pulsating heat pipe is performed having different diameter and on left and right limb. Water is used as working fluid with filling ratio of 60%. Higher filling ratio is considered to avoid dry out condition, the liquid and vapor slugs are observed with contours of liquid volume fraction. Heating is done at the evaporator section and temperatures are visualized in the contours of wall temperature.

## 2. Geometry and Physical Attributes

### 2.1. Geometry

The geometry of single turn closed loop pulsating heat pipe with different limb diameter is prepared with Ansys design modeler. The geometry is slice to set the filling ratio of working fluid and to define the presence of liquid and air.

## 2.2. Physical Characteristics of PHP

The inner diameter (ID) of PHP is 2mm and outer diameter (OD) of 3mm at majority of the geometry. However, the left and right limb of PHP has different diameter. The left limb corresponds to an inner diameter of 2mm and right limb corresponds to an inner diameter of 1.5 mm. The different limb diameters are joined with converging and diverging section. Out of the total volume of tube, 11% of volume is occupied by the evaporator and 27% volume occupied by condenser.

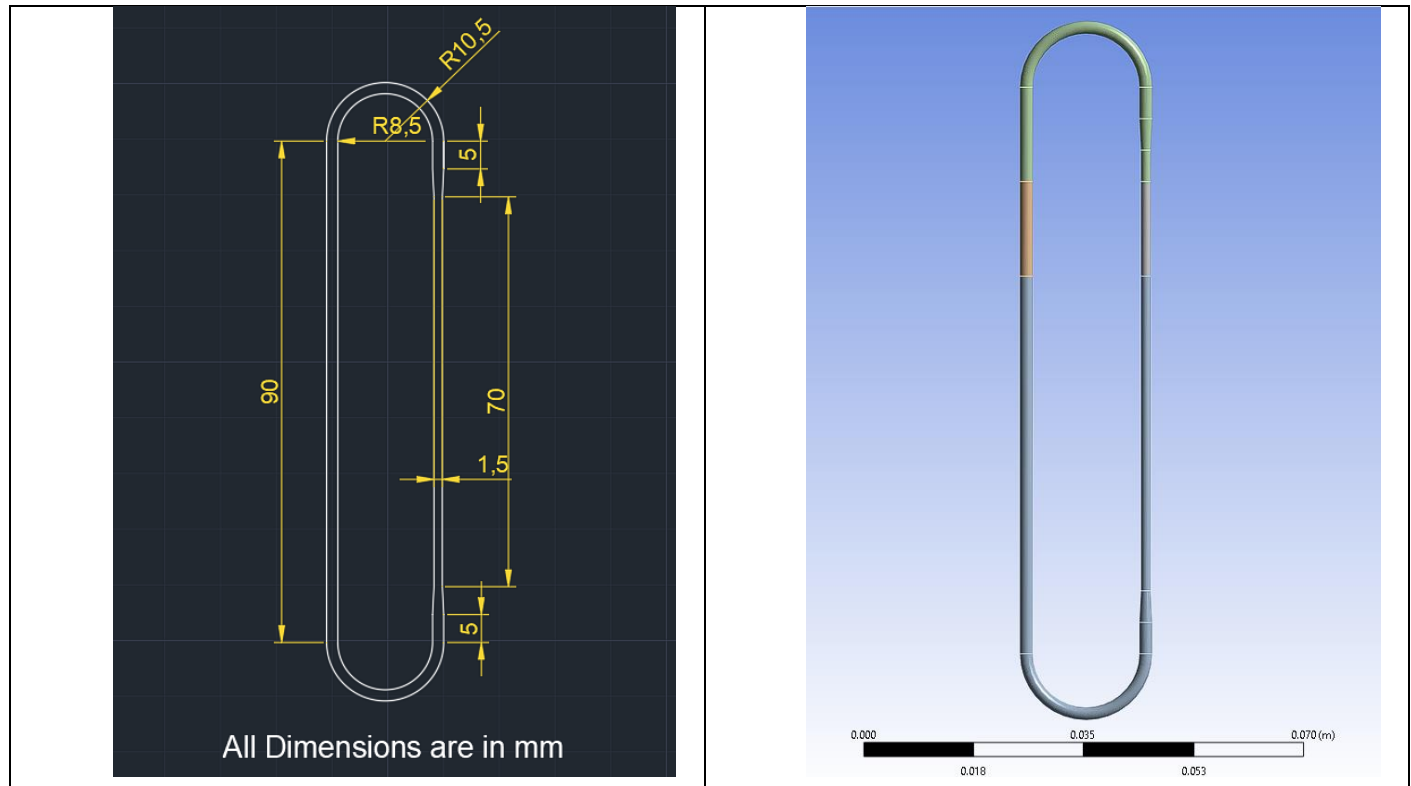


Fig 1: Schematic diagram of numerical model of PHP.

## 3. Mesh Generation and Independence Study

### 3.1. Details of mesh

The Mesh is generated with meshing tool available in Ansys workbench. The details of nodes and element corresponds to liquid, and air domain on 3D computational domain is as shown in the table 1.

Table 1: Details of nodes, element and volume occupied on 3D computational domain

Sr. No.	Domain	Nodes	Element	Volume in mm <sup>3</sup>	% of the Total Volume
1	Air	24216	21103	251.17	38.70%
2	Liquid	45305	40432	398.43	61.3%
3	All Domain	69521	61535	649.5	100%

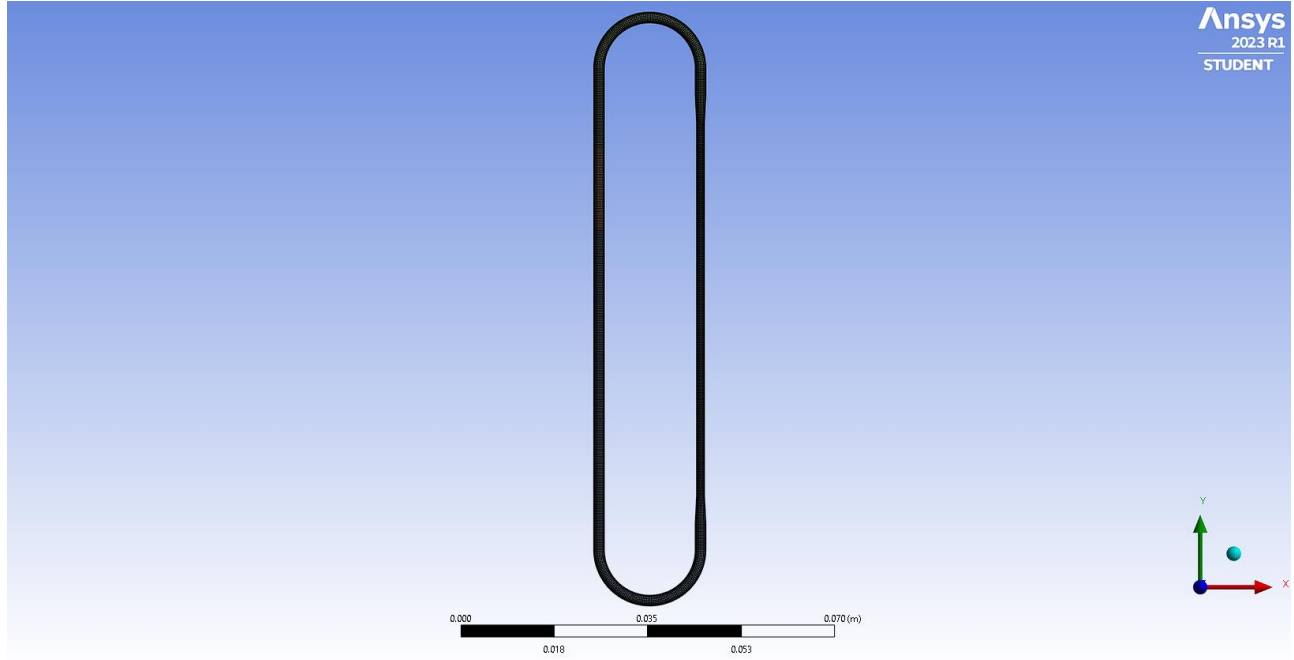


Fig 2: Mesh generated at evaporator, adiabatic and condenser section of PHP

### 3.2. Mesh Independent Study

To check the accuracy of CFD simulation it is necessary to perform the mesh independence study. The mesh is generated for three difference sizes i.e., course, medium and fine. The time required for CFD simulation depends on the mesh size selected. While proceeding for simulation it was ensured to have skewness near to '0' and orthogonal quality near to '1'. The mesh generated satisfying the above criterion is selected for simulation. The selection of mesh also ensured to keep the Courant Number to a lower value to avoid the divergence in the velocity field. CFD simulation is performed with student version of Ansys keeping in mind limitation nodes and element and computational time required.

## 4. Governing Equations and Boundary Conditions

### 4.1. Energy Equations Governing the Physics of Fluid Flow

The two-phase fluid flow in PHP with different limb diameter is numerically simulated by volume of fluid (VOF) method. The VOF method is useful to track the interface fluid flow. The subscripts "l" & "v" represent liquid and vapor slugs.

$$\frac{\partial(\alpha_v \rho_v)}{\partial t} + \nabla \cdot (\alpha_v \rho_v \mathbf{v}_v) = \dot{m}_{lv} - \dot{m}_{vl} \quad (1)$$

The momentum equation is solved throughout the domain Eq. (2) which is reliant on volume fractions of all the phases.

$$\frac{\partial}{\partial t} (\rho \mathbf{v}) + \nabla \cdot (\rho \mathbf{v} \mathbf{v}) = -\nabla P + \nabla \cdot [\mu (\nabla \mathbf{v} + \nabla \mathbf{v}^T)] + \rho \mathbf{g} + F_{vol} \quad (2)$$

The energy equation shared among the phases is shown in Eq. (3). Here,  $Sh$  is energy source caused by phase change.

$$\frac{\partial}{\partial t} (\rho E) + \nabla \cdot (\mathbf{v} (\rho E + P)) = \nabla \cdot (K \cdot \nabla T + (\bar{\tau} \cdot \mathbf{v})) + Sh \quad (3)$$

The thermal resistance of pulsating heat pipe can be obtained by

$$R_{th} = \frac{T_e - T_c}{Q} \quad (4)$$

#### 4.2. Model and Material Section

Multiphase volume of fluid model is used and energy equation is turned on, as the temperature variations are taking place. Number of eulerian phases are defined as water liquid and water vapor. Copper is selected as material of pipe due to its compatibility with water as working fluid. The k- $\epsilon$  model is used with enhanced wall treatment, thermal effect and curvature correction.

#### 4.3. Phase Definition on Computational Domain

Two phases are defined on the 3d computational domain, primary phase as water vapor (steam) and secondary phase as water liquid. Surface tension force modelling is taken into consideration with wall adhesion, surface tension coefficient of 0.0736 N/m. Mass transfer mechanism is set for evaporation of steam from water.

#### 4.4. Setting Cell Zone Conditions on Computational Domain

The operating pressure of 4000 Pa is specified. As there is gravity assisted flow of fluid from evaporator to the condenser section gravity of 9.81 m/s<sup>2</sup> is specified. Thermal boundary conditions are specified at evaporator section with temperature of 323 K and condenser temperature of 298 K. As the diameter is small capillary action takes place, contact angle of 20° is specified.

#### 4.5. Setting Initialization and Patch

Standard initialization is considered and water liquid is patched with 3D computational domain specified with water. The water vapor phase initially is zero meaning that only water liquid is present inside the capillary tube.

#### 4.6. Simulation Setup

Adaptive time steps are selected to avoid the problem of courant number (CFL) with time step size of 0.0005. Lower time steps prevent the divergence in velocity field. Contours of liquid volume fraction and contours of wall temperature are specified to visualized the result in post processor.

The table below demonstrate the importance of choosing an appropriate time step in numerical simulations. While smaller time steps enhance stability and accuracy, they also increase computational cost. A balance between stability and computational efficiency is critical for optimizing simulation performance. For a time step size of 0.1, the simulation diverges very quickly. This indicates that the time step is too large to capture the underlying physical phenomena accurately, leading to instability in the numerical solution. At a time step size of 0.01, the simulation also diverges, though it is slightly more stable compared to 0.1. The reduced time step size improves accuracy but is still insufficient to stabilize the simulation. With a time, step size of 0.001, the simulation performs better and diverges only after some time. This suggests that the time step is closer to the stability threshold but still not small enough for long-term accuracy and convergence. At a time step size of 0.0005, the simulation does not diverge and remains stable. However, this time step is very small, significantly increasing computational time, as the solver takes more iterations to progress through the same physical time period.

Table 3: Effect of time step size on velocity field.

Sr. No.	Time step size	Issue
1	0.1	Diverges very fast
2	0.01	Diverges
3	0.001	Diverges after some time
4	0.0005	Takes long time but never diverge

## 5. CFD Simulation

CFD Simulation is performed with water as working fluid, the contours of liquid volume fraction and contours of wall temperature are observed from the time step of “0” to time step of “300000”.

### 5.1. Contours of Liquid Volume Fraction

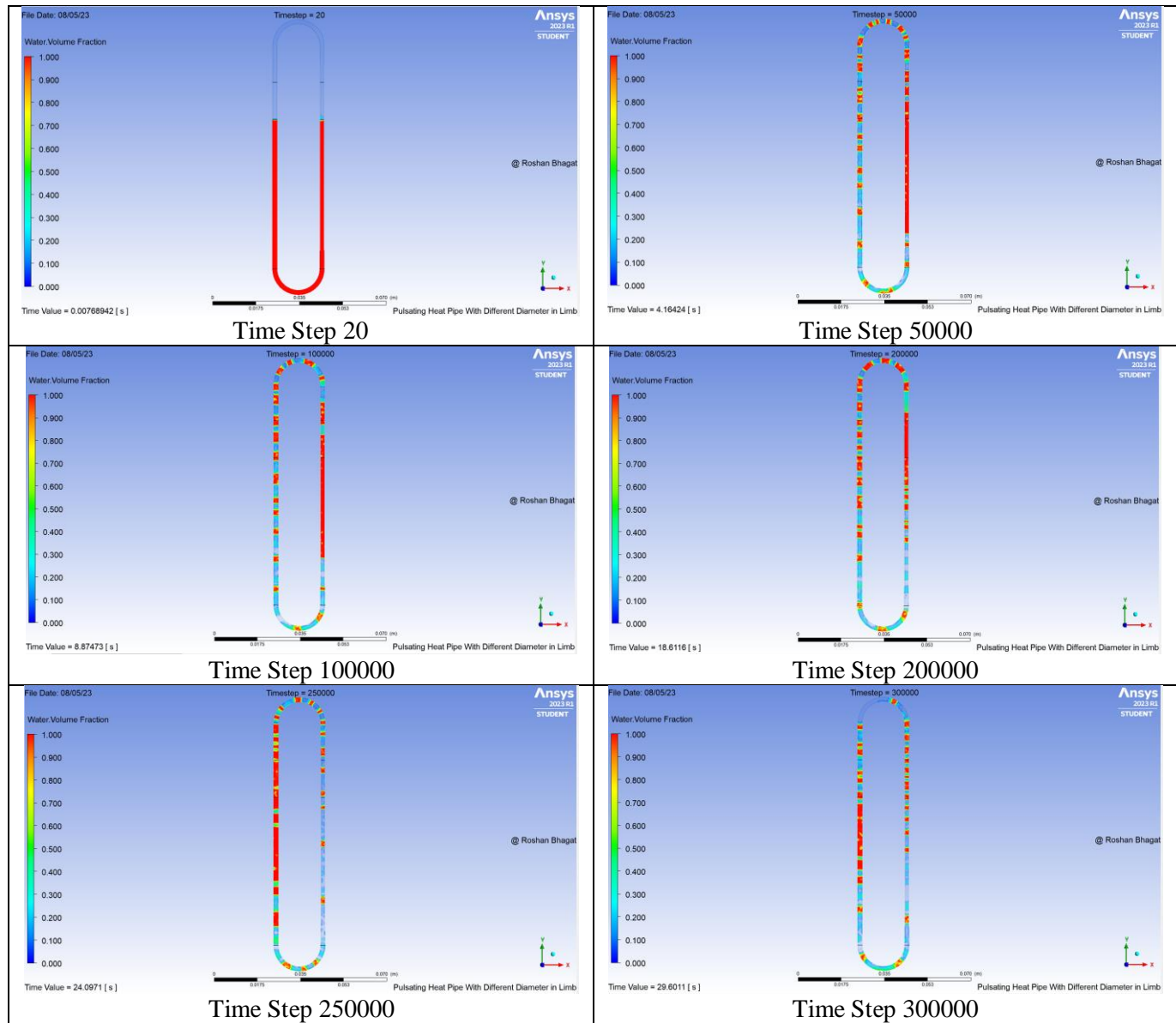


Fig 3: Contours of liquid volume fraction for PHP with different limb diameter

Figure 3 shows the contours of liquid volume fraction, at initial time step of 20 only liquid phase is present inside the tube, with increase in time step alternate liquid and vapor slugs are observed along the length of PHP, moving from left limb to the right limb up to time step of 225000. This visualization demonstrates the transient behaviour of the fluid at a specific time step (29.6011 seconds), providing insights into the heat transfer and flow characteristics of system.

## 5.2. Contours of Wall Temperature

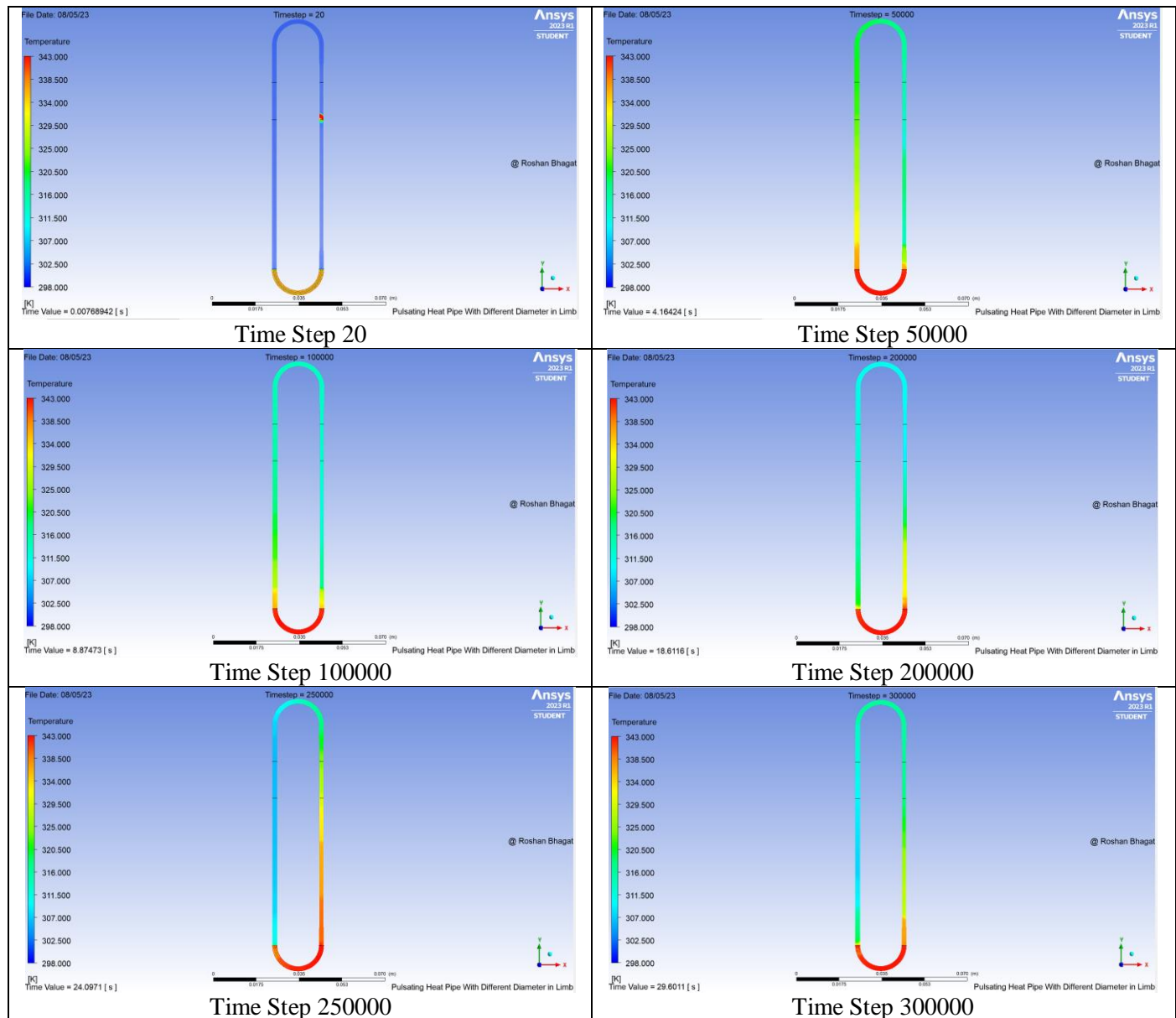


Fig 4: Contours of wall temperature for PHP with different limb diameter

## 5.3. CFD Results

This table presents the variation of temperature along the evaporator section of the right and left limbs in a pulsating heat pipe, measured at specific distances from a reference point. As the distance increases, the temperature decreases progressively in both limbs, indicating heat transfer and cooling along the evaporator section of pulsating heat pipe.

Table 4: Temperature of right and left limb in with CFD

Sr. No.	Distance [m]	Temperature [K] at right limb	Temperature [K] at left limb
1	0	339	333
2	0.01	337	318
3	0.02	327	309
4	0.03	326	307
5	0.04	324	308
6	0.05	322	309
7	0.06	318	310
8	0.07	317	312
9	0.08	317	313
10	0.09	317	314

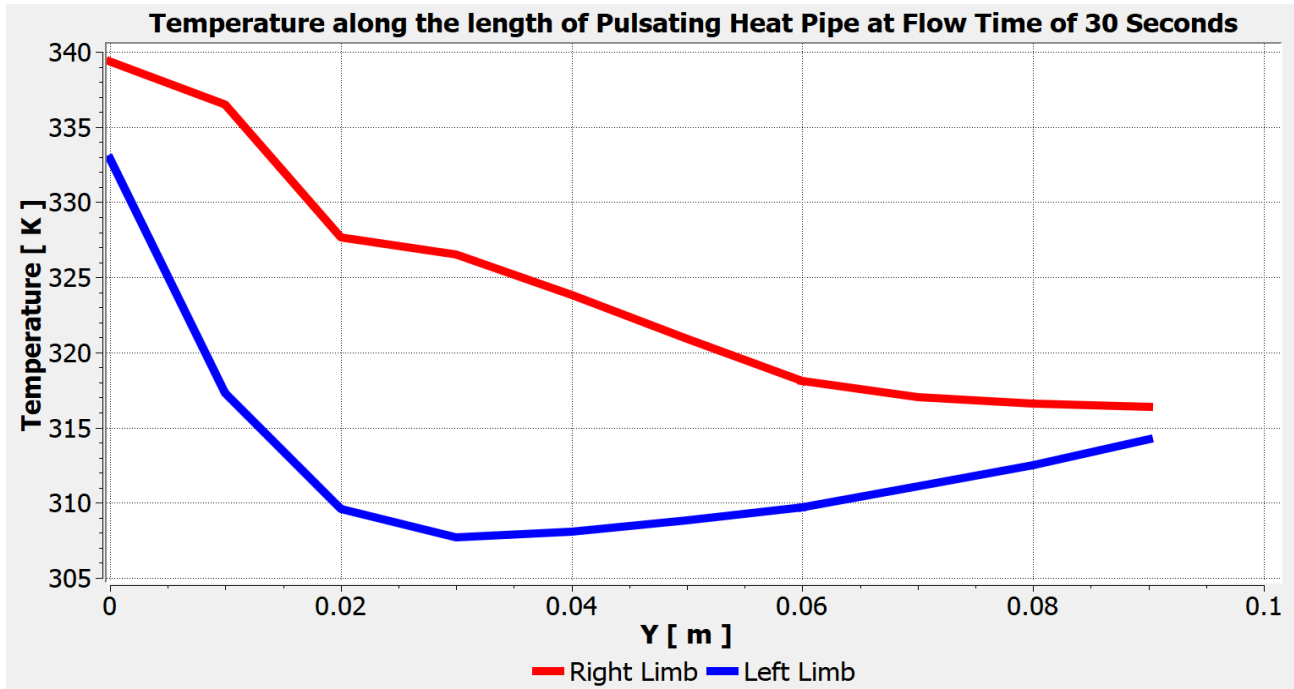


Fig 5: Contours of wall temperature along the length for PHP with different limb diameter

## 6. Validation with Experiment

### 6.1 Description of Experimental Setup

Experimental setup consists of PHP with different limb diameter. The temperature at evaporator and condenser section is measured with the help of digital laser thermometer. Heat input is provided into the heater. The maximum temperature of 343 K is recorded during the experimentation.

### 6.2 Experimental Result

The table presents experimental temperature measurements along the evaporator section of the right and left limbs of a pulsating heat pipe at specific distances. It shows that the right limb consistently has higher temperatures than the left limb, with both limbs exhibiting a general decrease in temperature as the distance from the reference point increases. This trend

highlights the heat transfer dynamics within the evaporator section, with temperature gradients indicating the dissipation of thermal energy.

Table 5: Experimental values of temperature at right and left limb.

Sr. No.	Distance [m]	Temperature [K] at right limb	Temperature [K] at left limb
1	0	335	330
2	0.01	337	324
3	0.02	335	318
4	0.03	330	315
5	0.04	320	312
6	0.05	327	316
7	0.06	325	320
8	0.07	322	319
9	0.08	322	320
10	0.09	320	310

### 6.3 Comparison of Experimental and CFD Result

The bar chart compares experimental and CFD results for the temperature distribution along the length of a pulsating heat pipe (PHP) with different limb diameters. It shows that the temperatures at the right limb are consistently higher than those at the left limb in both experimental and CFD results. The CFD predictions closely follow the experimental trends, validating the accuracy of the numerical model in capturing the thermal behavior of the PHP.

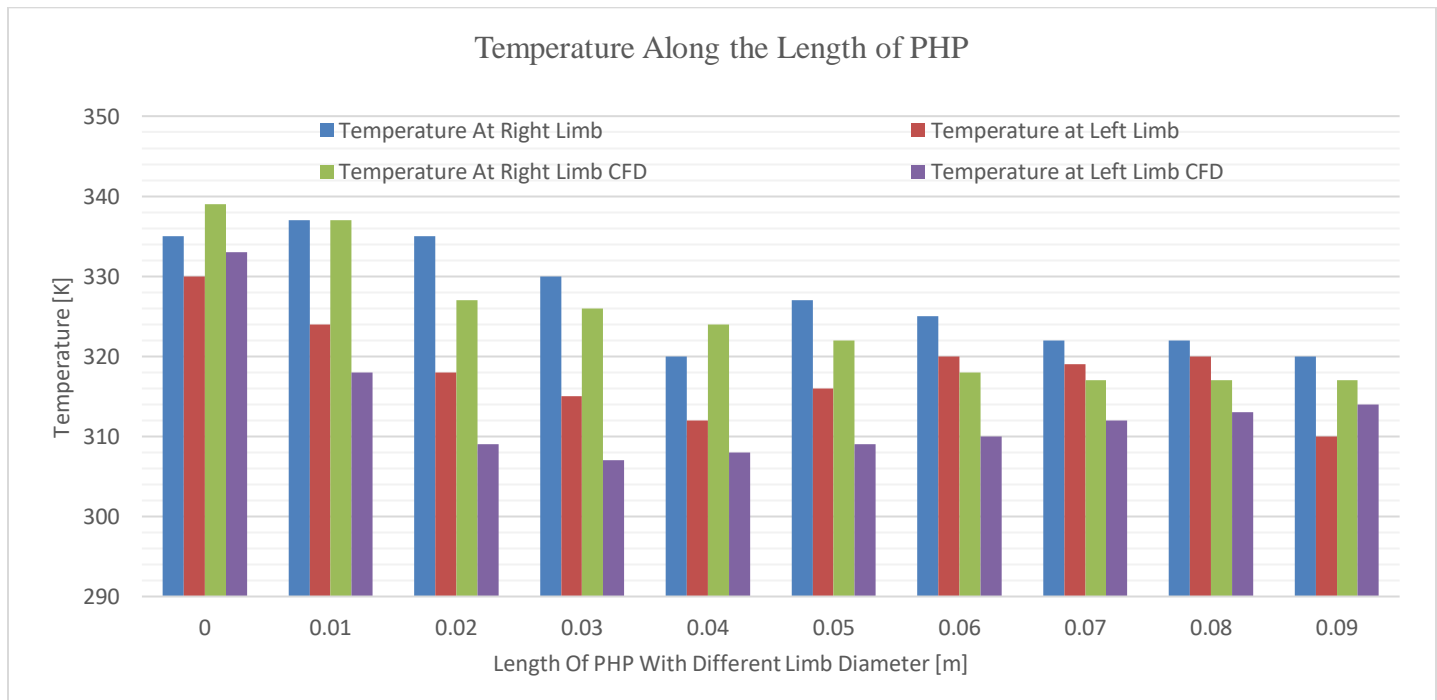


Fig 6: Comparison of experimental and CFD result for PHP with different limb diameter



## 7. Conclusion

After comparing the experimental and CFD result of PHP with different limb diameter following conclusions are made. The temperature generally decreases as the length of the PHP increases, indicating effective heat dissipation along the pipe. This trend is consistent for both the left and right limbs in both experimental data and CFD simulations. The CFD simulation data (gray and yellow bars) show good agreement with the experimental data (blue and orange bars), particularly at shorter lengths (0 to 0.03 meters). However, there are some deviations at longer lengths (beyond 0.06 meters), where the CFD results tend to show slightly lower temperatures compared to the experimental values. This suggests that the simulation may slightly underestimate the heat dissipation in longer sections. The temperature profiles for the left and right limbs are relatively similar, indicating symmetrical heat transfer performance in the PHP design. The symmetry observed in both the experimental and simulation results confirm the reliability of the PHP's design in maintaining uniform thermal performance across both limbs. There is a noticeable effect of limb diameter on the overall temperature distribution. Sections with smaller diameters tend to show slightly lower temperatures, indicating potentially enhanced heat transfer due to higher surface area-to-volume ratios. This observation suggests that optimizing the limb diameter could further enhance the thermal performance of the PHP. The chart indicates that both experimental and simulated data align closely, validating the accuracy of the CFD model used. The PHP demonstrates efficient thermal management, with effective cooling along its length, making it suitable for applications requiring efficient heat dissipation. Minimum variation in temperatures is observed at section near to the evaporator, and condenser for both right and left limb. At midway between the evaporator and condenser section the variation is minimum with few exceptions at distance of 0.02 and 0.06 m from evaporator. The simulation results show the minimum possibility of dry out condition as the vapor slug after rejecting heat from condenser section returns back to the evaporator section.

## Nomenclature

CLPHP	: Closed Loop Pulsating Heat Pipe	$\vec{v}$	: Velocity vector of the fluid (m/s)
PHP	: Pulsating Heat Pipe	P	: Pressure (Pa)
CFD	: Computational Fluid Dynamics	$\mu$	: Mixture dynamic viscosity (Pa·s)
CFL	Courant–Friedrichs–Lewy number	$(\nabla\vec{v})^T$	: Transpose of the velocity gradient tensor
ID	: Inner Diameter	$\vec{g}$	: Gravitational acceleration vector (m/s <sup>2</sup> )
OD	: Outer Diameter	$\vec{F}_{vol}$	: Volumetric body force (e.g., due to surface tension or external fields) (N/m <sup>3</sup> )
VOF	: Volume of Fluid	E	: Total energy per unit mass (includes internal, kinetic, and potential energy) (J/kg)
$\alpha_v$	: Volume fraction of the vapor phase	K	: Effective thermal conductivity of the mixture (W/m·K)
$\rho_v$	: Density of the vapor phase (kg/m <sup>3</sup> )	T	: Temperature (K)
$\vec{v}_v$	: Velocity vector of the vapor phase (m/s)	$\bar{\tau}$	: Shear stress tensor (Pa)
$\dot{m}_{lv}$	: Mass transfer rate from liquid to vapor due to evaporation (kg/m <sup>3</sup> ·s)	$S_h$	: Volumetric heat source due to phase change (W/m <sup>3</sup> )
$\dot{m}_{vl}$	: Mass transfer rate from vapor to liquid due to condensation (kg/m <sup>3</sup> ·s)	$R_{th}$	: Thermal resistance of the pulsating heat pipe (K/W)
t	: Time (Seconds)	$T_e$	: Evaporator temperature (K or °C)
$\nabla$	: Divergence operator (indicates flux out of a control volume)	$T_c$	: Condenser temperature (K or °C)
$\rho$	: Mixture density (depends on phase volume fractions) (kg/m <sup>3</sup> )	Q	: Heat input or heat transfer rate (W)

## References

- [1] B. Akachi H, "Structure of a heat pipe," U.S. Patent 4921041, 1990.
- [2] Zhou W, Li Y, Chen Z, Deng L, Gan Y, "A novel ultra-thin flattened heat pipe with biporous spiral woven mesh wick for cooling electronic devices," *Energy Conversion and Management* 2019; 180:769–83.  
<https://doi.org/10.1016/j.enconman.2018.11.031>
- [3] Bhagat Roshan, Deshmukh Samir, "Numerical analysis of passive two-phase fluid flow in a closed loop pulsating heat pipe," *Frontiers in Heat and Mass Transfer* 2021, vol.16, no 23. <http://dx.doi.org/10.5098/hmt.16.23>
- [4] Khandekar S, and Groll M, "On the Definition of Pulsating Heat Pipe," *Proceedings of 5<sup>th</sup> Minsk International Seminar (Heat Pipes, Heat Pumps and Refrigerators)*, Minsk, Belarus, 2003.
- [5] Wang H, Qu J, Peng Y, Sun Q, "Heat transfer performance of a novel tubular oscillating heat pipe with sintered copper particles inside flat-plate evaporator and high-power LED heat sink application," *Energy Conversion and Management* 2019; 189:215–22. <https://doi.org/10.1016/j.enconman.2019.03.093>
- [6] Liu X, Chen Y, "Fluid flow and heat transfer in flat-plate oscillating heat pipe," *Energy and Building* 2014; 75:29–42.  
<https://doi.org/10.1016/j.enbuild.2014.01.041>
- [7] Xu RJ, Zhang XH, Wang RX, Xu SH, Wang HS, "Experimental investigation of a solar collector integrated with a pulsating heat pipe and a compound parabolic concentrator," *Energy Conversion and Management* 2017; 148:68–77.  
<https://doi.org/10.1016/j.enconman.2017.04.045>
- [8] Lim J, Kim SJ, "Fabrication and experimental evaluation of a polymer-based flexible pulsating heat pipe," *Energy Conversion and Management* 2018; 156:358–64. <https://doi.org/10.1016/j.enconman.2017.11.022>
- [9] Patel VM, Mehta HB, "Channel wise displacement-velocity-frequency analysis in acetone charged multi-turn closed loop pulsating heat pipe," *Energy Conversion and Management* 2019; 195:367–83.  
<https://doi.org/10.1016/j.enconman.2019.05.014>
- [10] Bhagat Roshan, Watt K, "An experimental investigation of heat transfer capability and thermal performance of closed loop pulsating heat pipe with a hydrocarbon as working fluid," *Frontiers in Heat Pipe*, 2015 vol. 6, no 1.  
<http://dx.doi.org/10.5098/fhp.6.7>